The interplay between different stimuli in a 4D printed photo-, thermal-, and water-responsive liquid crystal elastomer actuator

Chemistry–A European Journal
Research Article
doi.org/10.1002/chem.202300648
Chemistry Europe
European Chemical Societies Publishing
www.chemeurj.org

Special Collection

The Interplay between Different Stimuli in a 4D Printed Photo-, Thermal-, and Water-Responsive Liquid Crystal Elastomer Actuator

Alessio Cremonini,[a] Jeroen A. H. P. Sol,[b] Albert P. H. J. Schenning,[b, c] Stefano Masiero,[a] and Michael G. Debije*[b, d]

Abstract: Multi-stimuli responsivity in 3D-printed objects is receiving much attention. However, the simultaneous interplay between different environmental stimuli is largely unexplored. In this work, we demonstrate direct ink writing of an oligomeric ink containing an azobenzene photo-switch with an accessible hydrogen bond allowing triple responsivity to light, heat, and water. The resulting printed liquid crystal elastomer performs multiple actuations, the specific response depending on the environmental conditions. Bilayer films formed by printing on a static substrate can rapidly change shape, bending almost 80 degrees if irradiated in air or undergoing a shrinkage of about 50% of its length when heated. The bilayer film assumes dramatically different shapes in water depending on combined environmental temperature and lighting conditions.

Introduction

Additive manufacturing (AM) – 3D printing, colloquially – has become popular for prototyping and fabrication of soft-actuators and other mechanical components; AM allows deposition of three-dimensional structures rapidly using a variety of materials.[1–4] Among 3D printing techniques, direct ink writing (DIW) represents an innovative orientation method for liquid crystals.[5] In recent years, different liquid crystal elastomer (LCE) devices have been fabricated using DIW to perform multiple roles in soft actuators.[6] LCEs have been designed to respond to external stimuli including light,[7–11] moisture,[12,13] temperature,[6,9] and magnetic fields.[14] Generally, these devices have been restricted to responding to a single trigger, while in natural environments devices are exposed to a number of stimuli simultaneously.

Light-triggered actuators are particularly interesting for their rapid response and their easy and non-invasive manner of address. Photo-actuation behavior is usually generated by introducing photo-responsive moieties in the polymer, such as azobenzene derivatives (often called "azos").[15] Azos are able to induce macroscopic changes in the shape of LCEs, even when present in low concentrations. Azo-containing polymers can be photo-triggered in different environments,[16,17] and have been widely used as a photoresponsive core in numerous liquid crystalline devices.[18–24] Recently, oligomers containing azobenzene-based monomers have been exploited as inks for DIW light-responsive devices.[9,25–27]

Photoisomerization of azobenzenes is affected by the chemical structure of the azobenzene core as well as their environment. In particular, heteroatoms and substituents on the aromatic rings connected to the –N=N– group have a strong influence on the rate of thermal return from the *cis* to the *trans* configuration.[28] The presence of a hydroxyl group in *ortho* position with respect to the –N=N– group leads to the formation of an intramolecular hydrogen bond and decreases the *cis* isomer half-life.[29–31] In this work, we describe the fabrication and performances of multi-responsive LCE actuators produced by DIW using ink containing an *ortho*-hydroxyazobenzene moiety designed to not only respond independently to water, light, and temperature, but generate novel actuation behavior through interplay of these stimuli.

[a] *A. Cremonini, S. Masiero*
Dipartimento di Chimica "Giacomo Ciamician"
Università di Bologna
v. S. Giacomo 11, 40126 Bologna (Italy)
[b] *J. A. H. P. Sol, A. P. H. J. Schenning, M. G. Debije*
Stimuli-responsive Functional Materials and Devices (SFD)
Department of Chemical Engineering and Chemistry
Eindhoven University of Technology (TU/e)
Groene Loper 3, 5612 AE Eindhoven (The Netherlands)
E-mail: m.g.debije@tue.nl
[c] *A. P. H. J. Schenning*
Institute for Complex Molecular Systems (ICMS)
Eindhoven University of Technology (TU/e)
Groene Loper 3, 5612 AE Eindhoven (The Netherlands)
[d] *M. G. Debije*
Interactive Polymer Materials (IPM)
Eindhoven University of Technology (TU/e)
Groene Loper 3, 5612 AE Eindhoven (The Netherlands)

Supporting information for this article is available on the WWW under https://doi.org/10.1002/chem.202300648

Special Collection *Part of a Special Collection for "2022 Cross-strait (Hong Kong and Macao) Polymer Liquid Crystal State and Supramolecular Ordered Structure Academic Symposium."*

Results and Discussions

LC oligomers used for the multi-responsive DIW actuators must include a multi-responsive photoswitch in the main chain compatible with the liquid crystalline ink. In this work, a diacrylate azobenzene monomer ((*E*)-6-(4-((4-((6-(acryloyloxy)hexyl)oxy)-2-hydroxyphenyl)diazenyl)phenoxy)hexyl acrylate) (**2**) was obtained via nucleophilic substitution (See Figures S1–S2 in the Supporting Information). This azo compound replaced 4,4′-bis(6-acryloyloxyhexyloxy)azobenzene in the main chain of previously reported DIW inks.[9] The chemical composition for the oligomer consists of reactive LC mesogen **1**, **2**, and the isotropic chain extender 3,6-dioxa-1,8-octanedithiol (**3**). The acrylate-terminated main chain LC oligomer was synthesized via a dimethylphenylphosphine (DMPP) catalyzed thiol-Michael addition reaction with a slight molar excess of acrylate versus thiol (1.1 to 1) (Figure 1). The ^{1}H NMR spectrum of the ink shows acrylate signals between δ 6.40–5.70 ppm and the presence of a hydroxyl group on the ring (Figure S3). Gel permeation chromatography (GPC) confirms the azobenzene residues were incorporated into the main chain oligomer (Figure S4) with number-average molecular weight $\approx$6900 g mol^{-1}. Differential scanning calorimetry (DSC) spectrum and polarized optical microscopy (POM) show a crystal-to-smectic phase transition ($T_{C/Sm}$) at $\approx -25\,^{\circ}$C, a smectic-to-nematic phase transition (Sm/N) at $\approx$42 °C, and a nematic-to-isotropic phase transition (N/I) at 76 °C (Figure S5).

The ink was used for DIW to fabricate uniaxially oriented films. The printing temperature was set in the nematic phase, at 60 °C. Lines printed on RT substrates at speeds $<$5 mm s^{-1} did not show alignment when viewed via POM. Lines printed with speeds 6–15 mm s^{-1} showed birefringence when viewed via POM, suggesting the LCs oriented along the printing direction (Figure 2A–B). Based on these observations, the printing speed was set to 12 mm s^{-1}.

Single layer 'stripes' of different dimensions (2×25 mm^2 to 5×25 mm^2) were printed on top of one of two substrates. The first were glass substrates coated with polyvinylpyrrolidone (PVP). The PVP acts as a sacrificial layer for generation of free-standing films for control purposes (Figure 2C). The second were 10 μm uniaxially stretched polyetherimide (PEI) foils, convenient, flexible, passive substrates for substrate-bound bilayer films.[32] The modulus of PEI is on the same order of magnitude as poly(ethylene terephthalate) (PET),[33] appropriate for bending by the LC elastomer.

After photopolymerization of the films by UV light, sol/gel fraction experiments revealed an average 87% gel fraction for the LCE, while, according to the IR spectrum, there were no

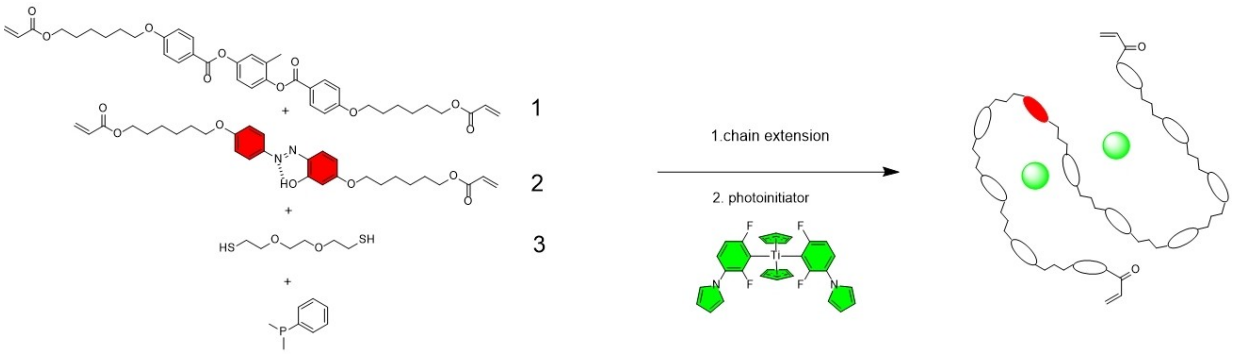

Figure 1. Chemical composition of the ink and synthesis of the oligomer: the reactive mesogens (**1**), the synthesized *o*-hydroxyl azobenzene (**2**, red), di-thiol spacer (**3**), catalyst and photoinitiator (green).

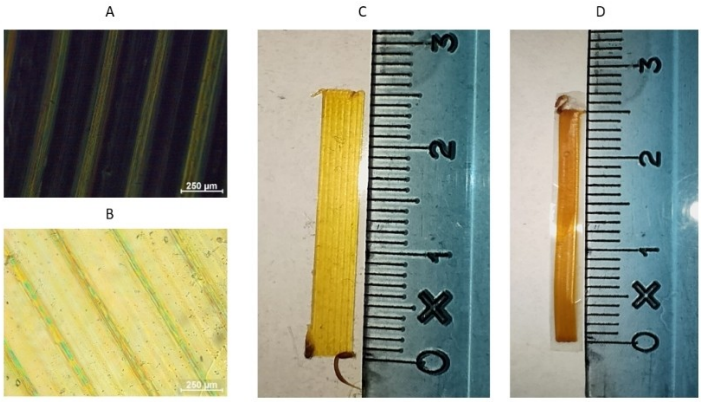

Figure 2. Polarized optical microscopy images of a film printed on glass oriented (A) parallel to one polarizer and (B) at 45° with respect to both polarizers. The scale bar represents 250 μm. (C) Polymer strips printed on PVP-covered glass and (D) on a PEI substrate.

discernable unreacted acrylate groups (see Figure S6). Using a contact profilometer, the average thickness of the oriented LC film was determined to be ≈100 μm. DSC measurements show a mesophase transition Sm/N at about 45 °C, and a N/I transition at ≈80 °C, see Figure S7. Free-standing films were obtained by detaching the LCE from the glass substrates by dissolving the PVP layer. For the substrate-bound samples, a laser cutter was used to cut the PEI supports around the LCE rectangles (Figure 2D) so the PEI film had 50% of its area covered by the LCE for enhanced actuation in the bilayer films.[34]

The response of the free-standing film and the substrate-bound samples to temperature was investigated using a convection oven. The free-standing film contracted along the deposition direction upon heating, similar to samples described in the literature:[6,9] longitudinal film shrinkage was quantified by plotting the fractional change in length as a function of temperature. As expected, different stages of the response were observed (see Figure S8): from 30 °C to ≈40 °C, below the nematic LC phase, minimal contraction was observed, followed by a reduction of length of about 20% from ≈45 °C (corresponding to the first mesophase transition in the DSC) to ≈80 °C. A second actuation occurred above 80 °C: the film contracts another 30%, so the overall contraction was around 50%. Above 85 °C, the LCs in the polymerized film are in the isotropic phase, and no additional changes in shape were registered. The film recovered its initial shape upon cooling the sample back to 30 °C. The substrate-bound film commences actuation at roughly the same temperature as the free-standing film as the LCs undergo mesophase transition (Figure 3), rolling up with the deposited film on the inside of the curl upon heating.

Photoactuation for a 4×25 mm^2 substrate-bound film in air was investigated using a 385 nm LED, by tracking vertical displacement of the tip of a film clamped and hung from a stand, under different light intensities with the deposited polymer film facing the light source, while the temperature of the film's exposed surface was registered with an IR thermal camera. The films bend with the LCE on the inside of the curl: increasing the light intensity (Figure 4A), and thus the heating

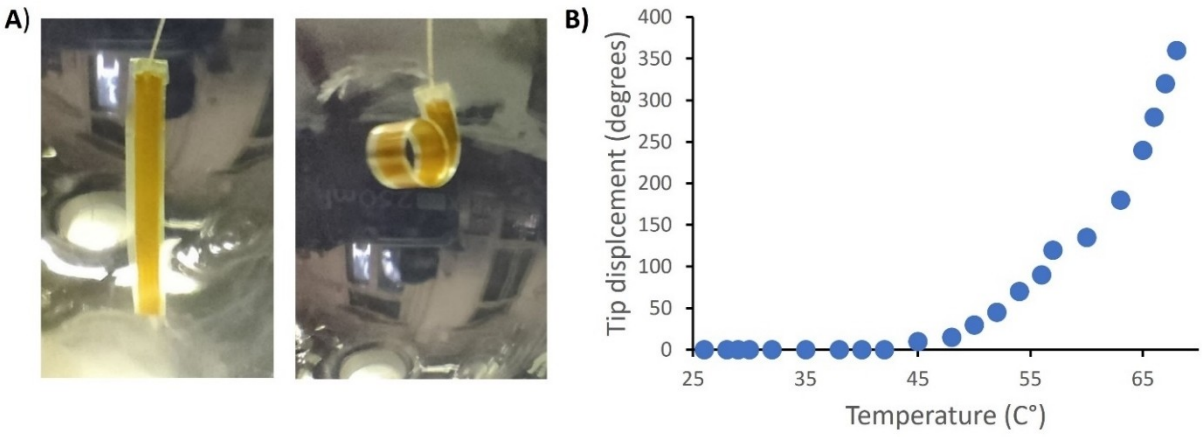

Figure 3. A) Photographs of the substrate-bound film at (left) 20 °C and (right) 60 °C, demonstrating the curling of the film B) Tip displacement of the substrate-bound film; above 45 °C the stripe starts contracting, rolling up with the LCE on the inside of the curl at 60 °C.

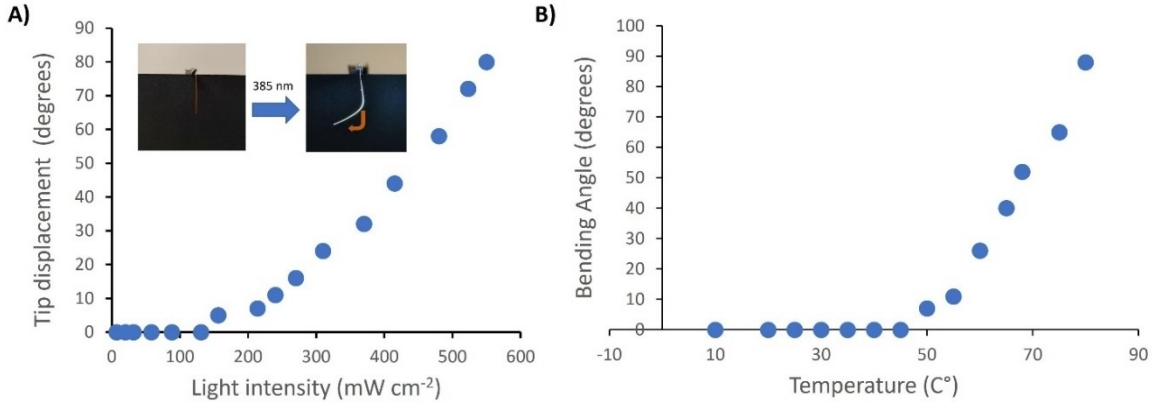

Figure 4. A) Bending angle from manual video analysis as a function of A) light intensity used during photoactuation. (Inset) Photoactuation of the substrate-bound film printed on PEI in air (printed film on the left side): bending triggered by 385 nm light incident from the left. and B) measured surface temperature of the substrate-bound film during photoactuation measured by the portable IR camera.

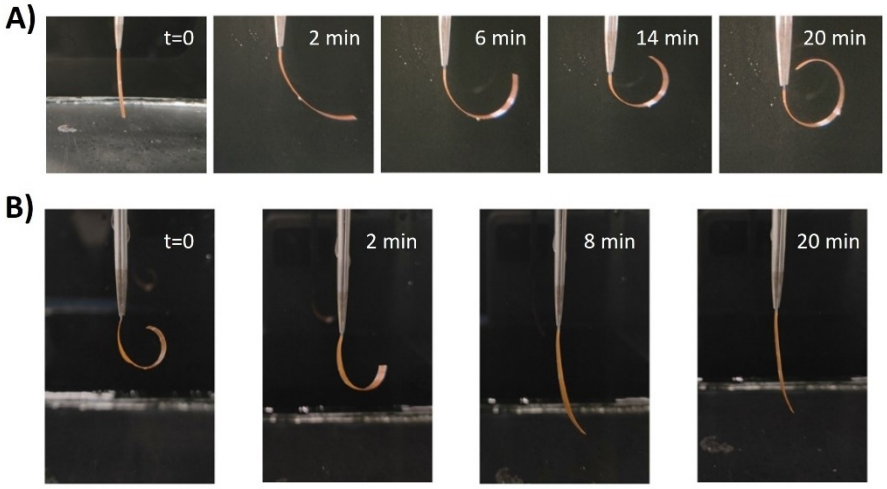

Figure 5. A) Actuation of the substrate-bound film underwater at 15 °C over a period of 20 min. The DIW polymer is on the left. B) Uncurling of the same film to its original shape after removal from water over a period of 20 min.

of the sample (Figure 4B), increased the maximum bending angle. The initial bend apparently releases some internal strain in the printed sample, for when the light is turned off the sample retreats rapidly, overshoots its initial state and forms a bent state in the opposite direction. A further 10 cycles of alternating UV light and darkness shows the film actuates regularly between these latter two states and did not show any obvious signs of fatigue (see Video S1 in the Supporting Information). The actuation is governed by photothermal effects:[16] no significant bending was observed when the measured film temperature was below 40 °C;[30] bending response was reminiscent of thermal actuation (Figure 3B), although the extent of bending was limited as the photothermal heating was confined to a smaller region and geometry prevented illumination when bending exceeded 90°.

When the free-standing film is submerged in water, no visible changes are observed. However, when the substrate-bound sample was submerged in water at RT, the bilayer film rolled with the substrate on the inside of the curl (Figure S9). The curling takes about 20 min to reach maximum displacement, and another 20 min to return to its original shape when removed from the water (the curling and uncurling of the substrate-bound film is seen in Figure 5).

The PEI substrate does not take up water. In contrast, the LCE likely does, causing the film to expand and force the bilayer to curl with the PEI substrate on the inside of the curl. When removed from the water, the water evaporates from the film, causing it to shrink and assume the initial shape for the bilayer. Samples were viewed under POM to ascertain if the liquid immersion disrupted the order of the LC: no obvious changes were observed (Figure S10). A weight increase of only 3 % was recorded after 20 min of immersion, sufficient to initiate bending.[35] FTIR spectra were used to evaluate if there were differences in carbonyl and ether bonds' stretching frequencies between the dry and the moist films, but no significant changes were observed, ruling out alterations in hydrogen bond arrangements. Furthermore, bilayer films containing the more common photo-responsive chromophore 4,4′-bis(6-acryloyloxyhexyloxy)azobenzene do not contain an intramolecular hydrogen bond,[9] and do not bend upon submersion in water at RT.

Increasing the water temperature led to contraction of the printed polymer: the substrate-bound film reaches a "straightened steady-state" between 32 and 42 °C and rolls on the polymer side on the inside of the curl above this temperature at the water uptake apparently is overcome by the thermal contraction (Figure 6). This result shows that at low temperature, water absorption and the expansion of the LCE layer dominates, whereas at high temperature the contraction of the LCE dominates.

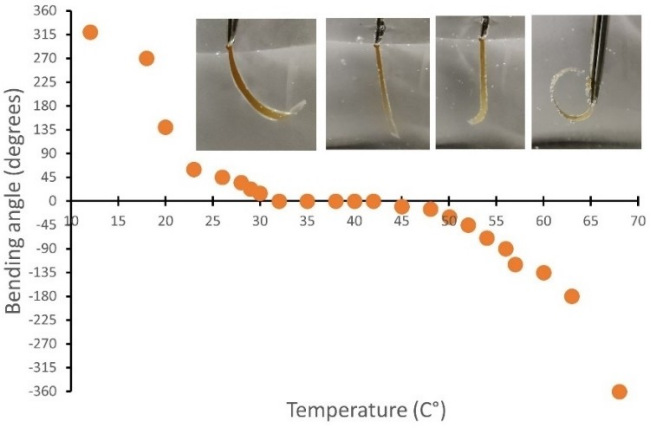

Figure 6. Underwater change in shape of substrate-bound actuator at different water temperatures. At low temperature the expansion of the polymer dominates leading to a bending to the substrate side (indicated by positive angles), while at higher temperatures the contraction of the polymers dominates making to device to bend to the polymer side (indicated by negative angles). (Inset) Photographs of sample in a round beaker displaying actuation at four temperature stages.

The concurrent interactions of all three stimuli – heat, light, and humidity – were also investigated. The bilayers films did not show any actuation when irradiated underwater with lower-intensity 385 nm light. However, replacing this with a high-power 365 nm lamp (1760 mW cm^{-2}) resulted in photothermal actuation and bending towards the light with the LCE on the inside of the curl. Once the high-intensity light is switched off, the return to the starting position is almost instantaneous: the polymer needs only few seconds to recover its initial shape due to the rapid heat loss to the water.[31] Bending and reversion occur at any environmental water temperature ranging from 0 °C to 50 °C (above this temperature, the bending of the film is at such a steep angle the tip moves to block the illumination). The maximum bending angles induced by illumination underwater vary: bending is greater at lower water temperatures and decreases as the water temperature increases as it becomes increasingly difficult to increase the film to temperatures greater than the surrounding water using the light (Videos S2 and S3). For a summary of actuation behavior of the substrate-bound films in both air and water environments, see Figure 7.

Conclusions

A novel oligomeric ink, in which the properties of photo-responsive moieties are influenced by a hydrogen bond, was synthesized to allow DIW fabrication of a tri-responsive thermal, light and water sensitive LCE film. The LCE performs multiple roles if triggered in different environments or conditions: it can rapidly change its shape up to a bend of almost 80° if irradiated in air or undergoes a shrinkage of about 50 % of its length when heated. Moreover, the film can assume different shapes in water depending on the environmental temperature and lighting conditions and could be used an amphibious "fast shape-recovering" actuator. This attempt to generate an LCE ink stimulated by multiple triggers opens new possibilities for fabrication of devices for soft robotics, such as light-driven swimming objects, where additional actuation capabilities are possible from the interplay of these varied stimuli.

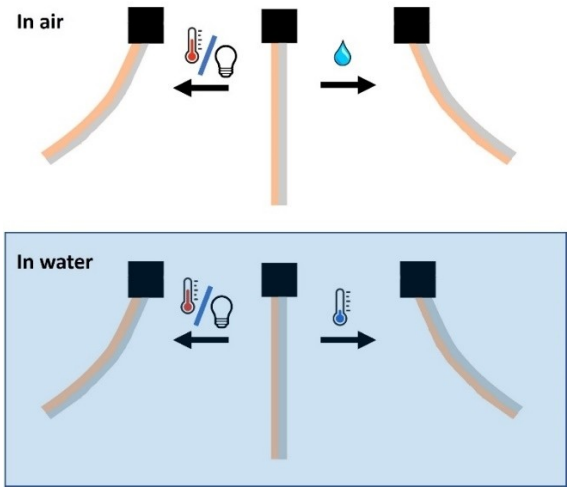

Figure 7. (Top) Actuation of the substrate-bound film in air (the LCE depicted as orange and the PEI substrates in gray). Thermal and photothermal actuation cause contraction of the LCE, resulting in bending with the LCE on the inside of the curl. Humidity causes the LCE to swell, resulting in bending with the LCE on the outside of the curl. (Bottom) Actuation of the substrate-bound film in water. In colder water, the LCE swells, and the film bends with the LCE on the outside of the curl. However, when the water is heated or the film is heated photothermally, the contraction of the LCE overcomes this swelling, the resulting contraction resulting in bending with the LCE on the inside of the curl.

Experimental Section

Materials: 1,4-bis(4-(6-acryloyloxyhexyloxy)benzoyloxy)-2-methylbenzene (**1**, "RM82") was purchased from Merck KGaA. 3,6-Dioxa-1,8-octanedithiol (**3**, DODT) and 1,8-diazabicyclo[5.4.0]undec-7-ene (DBU) were obtained from Sigma-Aldrich. Dimethylphenylphosphine (DMPP) was obtained from Sigma-Aldrich. Photoinitiator Irgacure 784 (bis(η^5-2,4-cyclopentadien-1-yl) bis(2,6-difluoro-3-(1*H*-pyrrol-1-yl)-phenyl)titanium) was purchased from BASF SE. Polyvinylpyrrolidone with an average molecular weight of 40,000 g mol^{-1} was purchased from Sigma-Aldrich. Dichloromethane (DCM) was obtained from Biosolve.

Synthesis of 1-(buta-1,3-dien-2-yloxy)-6-chlorohexane: 6-chlorohexan-1-ol (2.048 g, 15 mmol, 1 equiv.) was dissolved in 230 mL THF under argon atmosphere, stirred and cooled to 0 °C . Et_3N (4.186 mL, 30 mmol, 2 equiv.) was added and the mixture was left stirring for 30 min. Acryloyl chloride (1.22 mL, 15 mmol, 1 equiv.) was added dropwise leading to the production of a white precipitate. After 30 min the mixture was filtered, and the resulting crude solution was subjected to column chromatography (ethyl acetate:cyclohexane = 1:9 v/v). Rf-(product) = 0.82. The desired compound was obtained as a colorless oil with a yield of 86.6 % (2.45 g).

Synthesis of 4-((1*E*)-2-(4-hydroxyphenyl)diazen-1-yl)benzene-1,3-diol: 4-aminophenol (15 mmol, 1.6 g, 1 equiv.) was suspended in water (4.1 mL). The reaction mixture was stirred and cooled to 0 °C with an ice bath. Concentrated HCl (4.1 mL) was added dropwise dissolving 4-aminophenol. After 10 min of stirring, a solution of sodium nitrite (17 mmol, 1.14 g, 1.1 equiv.) in water (3.5 mL) was added dropwise to the mixture. The solution was stirred for 2 h at 0 °C. This solution was then added dropwise over 2 h to a solution of resorcinol (15 mmol, 1.6 g, 1 equiv.) dissolved in water (3.5 mL) and NaOH (37.5 mmol, 1.5 g, 2.5 equiv.) at 0 °C. Stirring was continued for 3 h while the mixture was warmed to room temperature. The solution was acidified with 1 M HCl and a red solid precipitate was obtained as the pure product with a yield of 85 %.

Synthesis of (*E*)-6-(4-((4-((6-(acryloyloxy) hexyl)oxy)-2-hydroxyphenyl)-diazenyl)phenoxy)hexyl acrylate (2): 4-((1*E*)-2-(4-hydroxyphenyl)diazen-1-yl)benzene-1,3-diol (0.43 mmol, 100 mg, 1 equiv.), 6-chlorohexylacrylate (0.86 mmol, 160 mg, 2 equiv.), potassium carbonate (0.86 mmol, 120 mg, 2 equiv.) and sodium iodide (catalytic concentration) were suspended in DMF (5 mL) under an argon atmosphere and heated at 80 °C for 24 h. The mixture was cooled, filtered, and concentrated under vacuum. Chloroform was added to the mixture and the organic layer was washed with saturated $NaHCO_3$ solution. The organic layer was dried over magnesium sulphate and concentrated. The crude mixture was subjected to chromatography column (dichloromethane: cyclohexane = 4:1 v/v), Rf(product) = 0.5. The fractions containing the product were pooled and dried under vacuum, the resulting orange powder was crystalized with methanol. The desired compound was obtained with a yield of 60 % (140 mg).

Oligomer synthesis: 1,4-bis(4-(6-acryloyloxyhexyloxy) benzoyloxy)-2-methylbenzene (**1**, 3.747 g, 1 equiv., 5.575 mmol), (*E*)-6-(4-((4-((6-(acryloyloxy)hexyl)oxy)-2-hydroxyphenyl)diazenyl)phenoxy)hexyl acrylate

(**2**, 0.300 g, 0.1 equiv., 0.557 mmol), 3,6-dioxa-1,8-octanedithiol (**3**, 1.014 g, 0.9 equiv., 5.575 mmol) where dissolved in 40 mL DCM under argon atmosphere in a one-necked flask. Argon was bubbled in the reactant solution at RT for 45 min, DMPP (0.0075 g) was added. The reaction was left stirring overnight at room temperature. The next day, Irgacure 784 (0.1 g, 0.033 equiv., 0.187 mmol) was added and the flask shielded from light to avoid premature polymerization. The mixture was poured in a PTFE evaporation dish and covered with aluminum foil punctured with little holes to evaporate the solvent overnight. The removal of the residual solvent was conducted in a vacuum oven at room temperature.

Preparation and deposition of the Ink: Direct ink writing was performed using a commercial 3D printer (Engine HR, Hyrel 3D, Norcross, GA, U.S.A.). The ink was loaded into a stainless-steel 10 cc reservoir at room temperature and extruded through a micronozzle (335 μm orifice diameter) at 60 °C reservoir temperature. The printing speed was 1.2 cm s^{-1}. Films ranging from 2×20 mm^2 to 5× 20 mm^2 were printed on top of PVP-coated glass and on 10 μm PEI substrates. The printing path was controlled by a G-code generated by the printer software. The distance between the deposited lines was set to 0.28 mm, while the distance between nozzle and the bed was 110 μm. After printing, samples were photopolymerized under nitrogen at room temperature with 40 mW cm^{-2} of 530 nm collimated light LED (ThorLabs), the power controller (ThorLabs DC4104) used to tune the intensity. After exposure for 2 h, in which the sample was flipped every 30 min, the film's thickness and birefringence were characterized via a profilometer system and a microscope, respectively. To obtain a free-standing film, the PVP layer was dissolved by immersing the sample in water at room temperature and subsequently dried at room temperature overnight, while films printed on PEI were cut with a laser cutter.

Characterization instruments: ^{1}H NMR spectra were collected on a 400 MHz Bruker Advance III HD spectrometer with deuterated chloroform or deuterated dichloromethane as solvent. GPC with was performed on a Shimadzu LC-2030.3D with 254 nm PDA and refractive index detectors to evaluate the number average molecular weight (M_n), weight average molecular weight (M_w), and dispersity ($Đ$) of oligomers using polystyrene (PS) with an average M_w of 350,000 g mol^{-1} as reference. DSC measurements were done using TA Instruments DSC Q2000. All microscopy images were taken with a Leica DM 2700 M equipped with two polarizers that were operated either crossed or parallel. The thickness of the film was determined via a Bruker DektakXT contact profilometer system. For actuation in air, films were placed at 20 cm distance from collimated UV light (λ_{LED} = 365 nm, Thorlabs M365L2). A camera (Olympus OM-D E-M10 Mk III) was used to record the light-driven deformation. The temperature of the surface of the film was measured using a Gobi camera from Xenics. Underwater actuation was conducted inside a transparent beaker. Underwater actuation was conducted inside a transparent beaker; the water temperature was controlled by a hot plate connected to a thermocouple (Nika). The UV lamp (Hamamatsu LC–L1V3, 365 nm) was placed at 3 cm distance from the sample and the actuation was recorded with the same camera.

Conflict of Interests

The authors declare no conflict of interest.

Data Availability Statement

The data that support the findings of this study are available from the corresponding author upon reasonable request.

[1] R. L. Truby, J. A. Lewis, *Nature* **2016**, *540*, 371–378.
[2] J.-Y. Lee, J. An, C. K. Chua, *Appl. Mater. Today* **2017**, *7*, 120–133.
[3] V. Mechtcherine, F. P. Bos, A. Perrot, W. R. L. da Silva, V. N. Nerella, S. Fataei, R. J. M. Wolfs, M. Sonebi, N. Roussel, *Cem. Concr. Res.* **2020**, *132*, 106037.
[4] S. Mantihal, R. Kobun, B.-B. Lee, *Int. J. Gastron. Food Sci.* **2020**, *22*, 100260.
[5] M. del Pozo, J. A. H. P. Sol, A. P. H. J. Schenning, M. G. Debije, *Adv. Mater.* **2022**, *34*, 2104390.
[6] M. López-Valdeolivas, D. Liu, D. J. Broer, C. Sánchez-Somolinos, *Macromol. Rapid Commun.* **2018**, *39*, 3–9.
[7] Y. Zhang, L. Huang, H. Song, C. Ni, J. Wu, Q. Zhao, T. Xie, *ACS Appl. Mater. Interfaces* **2019**, *11*, 32408–32413.
[8] A. Nishiguchi, H. Zhang, S. Schweizerhof, M. F. Schulte, A. Mourran, M. Möller, *ACS Appl. Mater. Interfaces* **2020**, *12*, 12176–12185.
[9] M. del Pozo, L. Liu, M. Pilz da Cunha, D. J. Broer, A. P. H. J. Schenning, *Adv. Funct. Mater.* **2020**, *30*, 2005560.
[10] O. M. Wani, H. Zeng, A. Priimagi, *Nat. Commun.* **2017**, *8*, 15546.
[11] S. Huang, Y. Huang, Q. Li, *Small Struct.* **2021**, *2*, 2100038.
[12] J. A. H. P. Sol, L. G. Smits, A. P. H. J. Schenning, M. G. Debije, *Adv. Funct. Mater.* **2022**, *32*, 2201766.
[13] O. M. Wani, R. Verpaalen, H. Zeng, A. Priimagi, A. P. H. J. Schenning, *Adv. Mater.* **2019**, *31*, 1805985.
[14] P. Zhu, W. Yang, R. Wang, S. Gao, B. Li, Q. Li, *ACS Appl. Mater. Interfaces* **2018**, *10*, 36435–36442.
[15] G. Wang, J. Zhang, *J. Photochem. Photobiol. C* **2012**, *13*, 299–309.
[16] M. Pilz da Cunha, E. A. J. van Thoor, M. G. Debije, D. J. Broer, A. P. H. J. Schenning, *J. Mater. Chem. C* **2019**, *7*, 13502–13509.
[17] T. J. White, *J. Polym. Sci. Part B* **2018**, *56*, 695–705.
[18] K. M. Lee, T. J. White, *Polymer* **2011**, *3*, 1447–1457.
[19] M. Yamada, M. Kondo, J. I. Mamiya, Y. Yu, M. Kinoshita, C. J. Barrett, T. Ikeda, *Angew. Chem. Int. Ed. Engl.* **2008**, *47*, 4986–8.
[20] M. Pilz da Cunha, H. S. Kandail, J. M. J. Den Toonder, A. P. H. J. Schenning, *Proc. Natl. Acad. Sci. U. S. A.* **2020**, *117*, 17571–17577.
[21] D. Sun, J. Zhang, H. Li, Z. Shi, Q. Meng, S. Liu, J. Chen, X. Liu, *Polymer* **2021**, *13*, 1889.
[22] L. Dong, Y. Zhao, *Mater. Chem. Front.* **2018**, *2*, 1932–1943.
[23] S. L. Oscurato, M. Salvatore, P. Maddalena, A. Ambrosio, *Nanophotonics* **2018**, *7*, 1387–1422.
[24] T. J. White, D. J. Broer, *Nat. Mater.* **2015**, *14*, 1087–1098.
[25] J. A. H. P. Sol, R. F. Douma, A. P. H. J. Schenning, M. G. Debije, *Adv. Mater. Technol.* **2023**, *8*, 2200970.
[26] L. Ceamanos, Z. Kahveci, M. Lopez-Valdeolivas, D. Liu, D. J. Broer, C. Sanchez-Somolinos, *ACS Appl. Mater. Interfaces* **2020**, *12*, 44195–44204.
[27] S. J. D. Lugger, L. Ceamanos, D. J. Mulder, C. Sánchez-Somolinos, A. P. H. J. Schenning, *Adv. Mater. Technol.* **2023**, *8*, 2201472.
[28] S. Crespi, N. A. Simeth, B. König, *Nat. Rev. Chem.* **2019**, *3*, 133–146.
[29] J. Garcia-Amorós, A. Sánchez-Ferrer, W. A. Massad, S. Nonell, D. Velasco, *Phys. Chem. Chem. Phys.* **2010**, *12*, 13238–13242.
[30] A. H. Gelebart, D. J. Mulder, M. Varga, A. Konya, G. Vantomme, E. W. Meijer, R. L. B. Selinger, D. J. Broer, *Nature* **2017**, *546*, 632–636.
[31] J. Garcia-Amorós, D. Velasco, *Phys. Chem. Chem. Phys.* **2014**, *16*, 3108–3114.
[32] R. C. P. Verpaalen, M. Pilz da Cunha, T. A. P. Engels, M. G. Debije, A. P. H. J. Schenning, *Angew. Chem. Int. Ed.* **2020**, *59*, 4532–4536; *Angew. Chem.* **2020**, *132*, 4562–4566.
[33] M. Pilz da Cunha, Y. Foelen, R. J. H. van Raak, J. N. Murphy, T. A. P. Engels, M. G. Debije, A. P. H. J. Schenning, *Adv. Opt. Mater.* **2019**, *7*, 1801643.
[34] M. del Pozo, J. A. H. P. Sol, S. H. P. van Uden, A. R. Peeketi, S. J. D. Lugger, R. K. Annabattula, A. P. H. J. Schenning, M. G. Debije, *ACS Appl. Mater. Interfaces* **2021**, *13*, 59381–59391.
[35] R. C. P. Verpaalen, A. E. J. Souren, M. G. Debije, T. A. P. Engels, C. W. M. Bastiaansen, A. P. H. J. Schenning, *Soft Matter* **2020**, *16*, 2753–2759.

Manuscript received: March 1, 2023
Accepted manuscript online: April 13, 2023
Version of record online: May 5, 2023